*Advanced Robotics*, Vol. 21, No. 7, pp. 751–770 (2007)

Also available online - www.brill.nl/ar

*Full paper*

# Fast model–image registration using a two-dimensional distance map for surgical navigation system

YUMI IWASHITA [1,*], RYO KURAZUME [1], KOZO KONISHI [2], MASAHIKO NAKAMOTO [3], NAOKI ABURAYA [3], YOSHINOBU SATO [3], MAKOTO HASHIZUME [2] and TSUTOMU HASEGAWA [1]

[1] *Kyushu University, 744 Motooka, Nishi-ku, Fukuoka, Japan*
[2] *Kyushu University, 3-1-1, Maidashi, Higashi-ku, Fukuoka, Japan*
[3] *Osaka University, 2-2, Yamada-oka, Suita, Osaka, Japan*

Received 2 June 2006; accepted 21 September 2006

**Abstract**—This paper presents a new registration algorithm of two-dimensional (2-D) color images and 3-D geometric models for the navigation system of a surgical robot. A 2-D–3-D registration procedure is used to precisely superimpose a tumor model on an endoscopic image and is, therefore, indispensable for the surgical navigation system. Thus, the performance of the 2-D–3-D registration procedure influences directly the usability of the surgical robot operating system. One of the typical techniques that has been developed is the use of external markers. However, the accuracy of this method is reduced by the breathing or heartbeat of the patient, as well as other unknown factors. For precise registration of 3-D models and 2-D images without external markers or special measurement devices, a new registration method is proposed that utilizes the 2-D images and their distance maps as created by the Fast Marching Method. Here, we present results of fundamental experiments performed using simulated models and actual images of the endoscopic operation.

*Keywords*: Two-dimensional–three-dimensional registration; Fast Marching Method; robust M-estimator; robotic surgery.

## 1. INTRODUCTION

Development work on a practical surgical robot system is proceeding with the goal of a minimally invasive surgical operation and a favorable postoperative process. Figure 1 shows the 'da Vinci' surgical robot system manufactured by Intuitive Surgical.

In general, the surgical robot system is composed of two main components, a manipulation system and a navigation system.

*To whom correspondence should be addressed. E-mail: yumi@irvs.is.kyushu-u.ac.jp

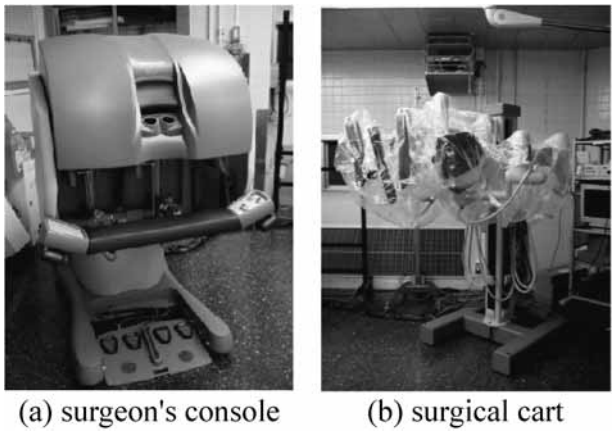


**Figure 1.** The 'da Vinci' surgical robot system.

The manipulation system of 'da Vinci' is the master–slave manipulator system. The slave manipulator consists of three arms: two 7-d.o.f. manipulators and one 5-d.o.f. camera holder. The manipulators are used to hold and operate several types of forceps, which can be replaced according to the purpose of the operation. The camera holder is used to control the position of an endoscope, which is equipped with two CCD cameras. Captured stereo images of internal organs are displayed on two LCDs in the surgeon's control console and provide stereognostic perception to the operator. The operator is able to control the forceps and the endoscope quite intuitively using the stereognostic perception.

Our navigation system for 'da Vinci' is designed to assist an operator by presenting the proper operation procedure to be performed and displaying the patient's information related to the operation [1]. Another main function of the navigation system is to display the invisible internal structure of an organ, the location of a tumor or the distribution of critical blood vessels in the endoscope image with a high degree of realism. The operator can intuitively obtain useful information from these realistic images so that the operation is performed smoothly.

The virtual images of an organ or the distribution of blood vessels are created from three-dimensional (3-D) geometric models, which are obtained using medical imaging devices such as computerized tomography (CT) or magnetic resonance imaging (MRI) beforehand. The obtained 3-D geometric models are projected onto the image plane of the endoscope and are superimposed on 2-D images of the target organs. The performance of this procedure directly influences the usability of the surgical robot operating system. Thus, the registration of 2-D images and 3-D geometric models has to be performed as precisely as possible.

Several registration techniques of 2-D images and 3-D geometric models have been proposed. One typical technique is the use of external markers to calibrate the coordinate systems fixed on the patient's body and the endoscope. In this method, the position of several markers, attached to the skin of the trunk and the endoscope,

are measured by an external optical device. The calibration calculation is then performed to determine the relative positions of these two coordinate systems. After calibration, the 3-D geometric models of organs are projected onto the 2-D images taken from the endoscope based on the standard position information of the organ in the patient's body. Therefore, the accuracy of this method is reduced if the organ moves away from the estimated position in the body due to the breathing or heartbeat of the patient, or other unknown factors.

The present paper introduces a new registration algorithm of 2-D color images and 3-D geometric models without external markers or special measurement devices. The proposed method utilizes the 2-D images and their distance maps as created by the Fast Marching Method, and it is possible to determine the precise relative positions of 2-D images and 3-D models. Since the registration process can be executed at quite a high speed using actual images, the registration accuracy is expected to be higher than that of the conventional method using external markers, even if the position of the organ is disturbed by the breathing or heartbeat of the patient, or other factors.

After an overview of previous works in Section 2, we will present a short introduction of the Fast Marching Method, which is utilized for the fast construction of a distance map, in Section 3. A detailed description of the new 2-D–3-D registration algorithm is presented in Section 4. Finally, in Section 5, we present the results of fundamental experiments using actual images of the endoscopic operation.

## 2. RELATED WORKS

For the alignment of a 2-D color image and a 3-D geometric model, Viola proposed a technique based on a statistical method [2]. This method evaluated the mutual information between the 2-D image and the image of the 3-D model based on the distribution of intensity. Allen *et al.* [3] also proposed a method using the intersection lines of several planes extracted from the range data and the color edges. These methods work well on surfaces with little albedo variance, but are easily trapped in local minima on surfaces with rich textures.

Range sensors often provide reflectance images as side products of range images. This 2-D reflectance image is aligned with the 3-D range image because both images are obtained through the same receiving optical device. Therefore, we can utilize the 2-D reflectance image to solve the 2-D–3-D registration problem instead of the original 3-D model. By using the 2-D reflectance image, the 2-D–3-D problem is modified to obtain a simple 2-D–2-D problem. Kurazume *et al.* [4] proposed a registration algorithm using the reflectance image and the 2-D texture image. In their method, a number of photometric edges extracted from both images were registered and the relative positions are determined using a robust M-estimator. Elstrom *et al.* [5] and Umeda *et al.* [6] also proposed methods using the reflectance image and the texture image. However, organs do not have rich texture on their surfaces and there are also differences in textures between individuals. Therefore,

texture-based methods are quite difficult to use for the 2-D–3-D registration problem of the surgical navigation system.

A number of registration techniques using a silhouette image or a contour line have been proposed. Lensch *et al.* [7, 8] proposed a silhouette-based approach, in which he used the XOR value of silhouette images of a 2-D image and a 3-D model to evaluate registration error. The Downhill Simplex Method was used for the convergent calculation of the 2-D–3-D registration. In the contour-based approach, the error is computed as the sum of the distances between points on a contour line in a 2-D image and on a projected contour line of a 3-D model [9, 10]. Since the number of point correspondences between both contours has to be determined for calculating the registration error, these algorithms are computationally expensive.

The proposed 2-D–3-D registration algorithm is a contour-based approach. However, instead of point correspondence, we adopt a distance map for evaluating the registration error. Therefore, once the distance map is created, the proposed algorithm runs faster than the conventional point-based approach [9, 10]. In addition, since the distance map can be created quite rapidly using the Level Set Method referred to as the Fast Marching Method, the proposed method can track an object continuously, even if the object moves.

## 3. FAST MARCHING METHOD FOR RAPID CONSTRUCTION OF A DISTANCE MAP

Before describing the proposed registration algorithm, the Fast Marching Method proposed by Sethian [11, 12], which is utilized for the fast construction of a distance map in the proposed method, is briefly introduced.

The Fast Marching Method [11, 12] was initially proposed as a fast numerical solution of the Eikonal equations ($|\nabla T(i, j)|\ F = 1$, where $T(i, j)$ is the arrival time of a front at a grid point $(i, j)$ and $F$ is a speed function). In general, since this equation is solved using a convergent calculation, a long time is required to obtain a proper solution. However, by adding a restriction such that a sign of the speed function $F$ is invariant, the Fast Marching Method solves the Eikonal equation quite rapidly in a straightforward manner. In this method, the arrival time of a front at each point is determined in order from old to new.

First, the Fast Marching Method modifies the Eikonal equation to obtain the following difference equation:

$$\left(\max(D_{ij}^{-x}T, -D_{ij}^{+x}T, 0)^2 + \max(D_{ij}^{-y}T, -D_{ij}^{+y}T, 0)^2\right)^{1/2} = 1/F_{ij}, \qquad (1)$$

where:

$$D_{ij}^{-x}T = \frac{T(i, j) - T(i-h, j)}{h} \quad D_{ij}^{+x}T = \frac{T(i+h, j) - T(i, j)}{h}$$
$$D_{ij}^{-y}T = \frac{T(i, j) - T(i, j-h)}{h} \quad D_{ij}^{+y}T = \frac{T(i, j+h) - T(i, j)}{h} \qquad (2)$$

and $h$ is spacing of grids.

Next, since the arrival time is propagated in one direction from old to new, the point that holds the oldest arrival time in an entire region is chosen and the arrival time of the boundary at this point is determined from (1).

The concrete procedure is as follows:

Step 1 (Initialization). The entire region is divided into a number of grid points with a proper grid width. Before starting the calculation, all of the grid points are categorized into three categories (known, trial, far) according to the following procedure:

(i) The grid points belonging to the initial front (denote the boundary hereafter) are added to the category of known and the arrival time of these grid points is set to 0 ($T = 0$).

(ii) Among the four neighboring grid points of a grid point belonging to the category of known, that which does not belong to the category of known is categorized into to the category of trial and the arrival time of this grid point is calculated temporarily from the following equation: $T_{ij} = 1/F_{ij}$. In addition, the arrival time of these grid points is stored in a heap data structure using the heap sort algorithm in ascending order of $T$.

(iii) The grid points other than the above grid points are all categorized into the category of far and the arrival time is set to infinity ($T = \infty$).

Step 2. Choose the grid point $(i_{\min}, j_{\min})$ that is located at the top of the heap structure. This grid point has the smallest arrival time in the category of trial. Remove this grid point from the category of trial and the heap structure, and categorize it into the category of known. Run the 'downheap' algorithm to reconstruct the heap structure.

Step 3. Among the four neighboring grid points $((i_{\min} - 1, j_{\min}), (i_{\min} + 1, j_{\min}), (i_{\min}, j_{\min} - 1)$ and $(i_{\min}, j_{\min} + 1))$ of the selected grid point $(i_{\min}, j_{\min})$, the point that belongs to the category of far is changed to the category of trial.

Step 4. Among the four neighboring grid points of the selected grid point $(i_{\min}, j_{\min})$, the arrival time of the point that belongs to the category of trial is calculated using (1). Then, run the 'upheap' algorithm to reconstruct the heap area.

Step 5. If there is a grid point that belongs to the category of trial, then go to Step 2. Otherwise, the process is terminated.

This Fast Marching Method constructs a distance map of an entire region quite rapidly, which indicates the distance from the boundary (the initial position of the front) to a certain point. To construct the distance map, the speed function $F_{ij}$ in (1) is initially set to 1. Next, the arrival time of the front, $T$, is determined using the above procedure. Since the speed function is 1, $T$ indicates the distance from the boundary to the point. Figure 2 shows an example of the calculated distance map.

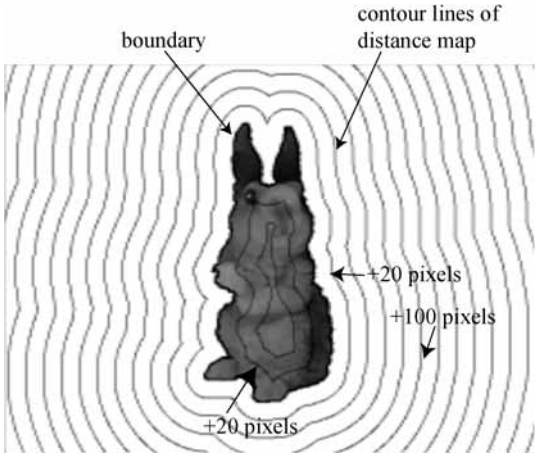


**Figure 2.** An example of a distance map calculation using the Fast Marching Method.

## 4. A NEW 2-D–3-D REGISTRATION ALGORITHM BASED ON THE DISTANCE MAP

This section describes in detail the proposed fast 2-D–3-D registration algorithm using the distance map. We assume that a 3-D geometric model of the target, such as the structure of an organ or a tumor, has been constructed by CT or MRI images beforehand and is represented by a number of triangular patches. A 2-D color image is also captured using a camera attached to an endoscope.

The proposed method is summarized as follows:

(i) First, the boundary of a target on the 2-D color image is detected using an active contour model (e.g., Snakes or the Level Set Method [13]).

(ii) Next, the distance map from the detected boundary on the 2-D image plane is constructed using the Fast Marching Method.

(iii) The 3-D geometric model of the target is placed at an arbitrary position and is projected onto the 2-D image plane.

(iv) Contour points of the projected image and their corresponding patches on the 3-D model are identified.

(v) A force is applied to the selected patch of the 3-D model in 3-D space according to the distance value obtained from the distance map at each contour point.

(vi) The total force and moment around the center of gravity (COG) of the 3-D model is determined using the robust M-estimator.

(vii) The position of the 3-D model is changed according to the total force and moment.

(viii) Repeat Steps (i)–(vii) until the sum of the difference between the projected contour of the 3-D model and the 2-D contour becomes less than a certain threshold or a maximum number of iterations is satisfied.

In the following sections, the above procedure is explained in further detail through examples.

### *4.1. Construction of the distance map*

Figure 3 shows the calculated distance map. First, a boundary is extracted from the color image using the Level Set Method [13]. Next, the distance map from this boundary is calculated using the Fast Marching Method explained in Section 3.

### *4.2. Fast detection of triangular patches of contour points in the 3-D model*

Figure 4 shows an example of the contour detection of the projected 3-D geometric model. The contour detection and identifying triangular patches on the 3-D model corresponding to points on the contour line are computationally expensive and time consuming. In the present implementation, we utilize the high-speed rendering function of the OpenGL hardware accelerator and execute these procedures quite rapidly.

The detailed algorithm is as follows. Initially, we assign different colors to each of the triangular patches in the 3-D model and draw the projected image of the 3-D model on the image buffer using the OpenGL hardware accelerator. The contour points of the 3-D model are detected by raster scanning of the image buffer. By reading the colors of the detected contour points, we can identify the corresponding

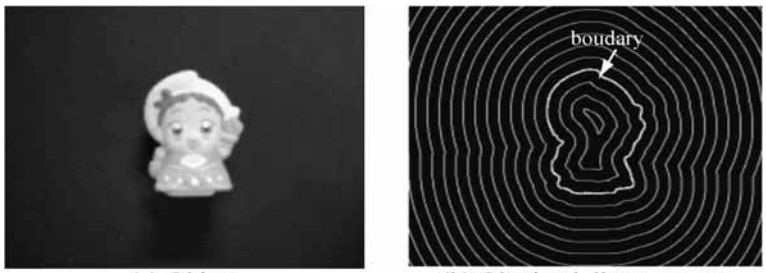


**Figure 3.** Detected boundary and distance map.

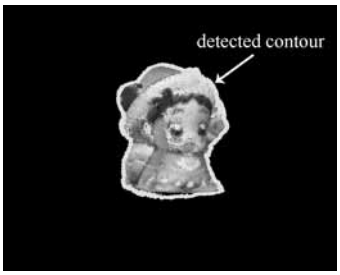


**Figure 4.** Contour detection of the 3-D geometric model.

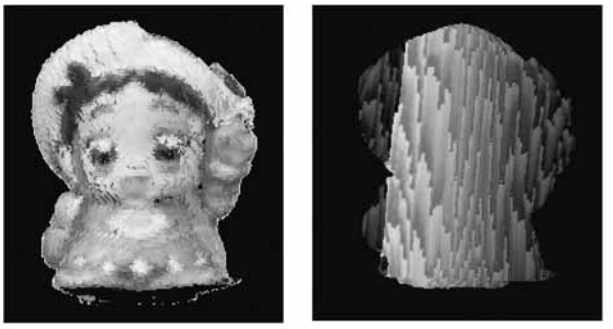


**Figure 5.** Detection of triangular patches of contour points.

triangular patches on the 3-D geometric model. Figure 5 shows the color image of the projected 3-D model with the patches of different colors.

### *4.3. Force and moment calculation using the M-estimator and determination of relative position*

After obtaining the distance map on the 2-D image and the list of the triangular patches of the 3-D model corresponding to the contour points, the force $f_i$ is applied to all of the triangular patches of the contour points (Fig. 6). The force $f_i$ is the vector perpendicular to the line of sight and the projection of $f_i$ onto the 2-D image plane coincides with $f_{\mathrm{DM}_i}$, which is the vector toward the direction of the steepest descent of the distance map (Fig. 7a). We assume that the magnitude of $f_{\mathrm{DM}_i}$ is proportional to the value on the distance map at the projected contour point of the 3-D model. Then, the total force and moment around the COG are calculated using the following equations, as shown in Fig. 7:

$$F = \sum_i \rho(f_i) \tag{3}$$

$$M = \sum_i \rho(r_i \times f_i), \tag{4}$$

where $r_i$ is a vector from the COG to the triangular patch $i$ and $\rho(z)$ is a particular estimate function.

In practice, a part of the target organ is occasionally hidden by other organs in the endoscopic image. In this case, the obtained boundary does not coincide with the projected contour of the 3-D model and the correct distance map cannot be obtained. Therefore, the robust M-estimator is used in the proposed system to ignore contour points with large errors. Let us consider the force $f_i$ and the moment $r_i \times f_i$ as an

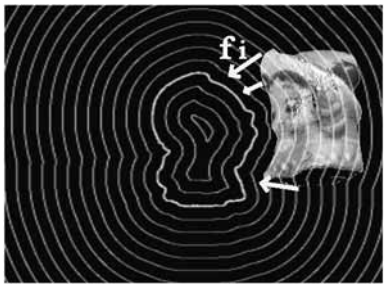


**Figure 6.** Application of the force $f$ to all of the triangular patches of the contour points.

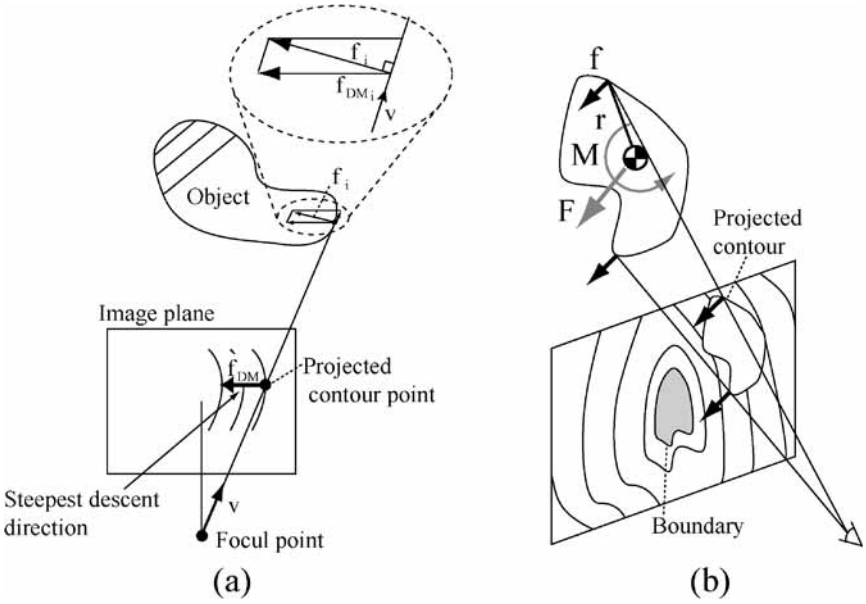


**Figure 7.** Force and moment around the COG.

error $z_i$. Then, we modify (3) and (4) as follows:

$$E(P) = \begin{pmatrix} F \\ M \end{pmatrix} = \sum_i \rho(z_i), \tag{5}$$

where $P$ is the position of the 3-D geometric model.

Position $P$ that minimizes $E(P)$ is obtained as follows:

$$\frac{\partial E}{\partial P} = \sum_i \frac{\partial \rho(z_i)}{\partial z_i} \frac{\partial z_i}{\partial P} = 0. \tag{6}$$

Here, in order to evaluate the error term, we define the weight function $w(z)$ as follows:

$$w(z) = \frac{1}{z}\frac{\partial \rho}{\partial z}. \tag{7}$$

From the above equation, we obtain the following weighted least-squares method:

$$\frac{\partial E}{\partial P} = \sum_i w(z_i) z_i \frac{\partial z_i}{\partial P} = 0. \tag{8}$$

In the present implementation, we adopt the Lorentzian function for the estimation function $\rho(z)$ and gradually minimize the error $E$ in (5) by the steepest descent method:

$$\rho(z) = \frac{\sigma^2}{2}\log(1 + (z/\sigma)^2) \tag{9}$$

$$w(z) = \frac{1}{1 + (z/\sigma)^2}. \tag{10}$$

The value $P$, which minimizes the error in (5), is the estimated relative position between the 2-D image and the 3-D geometric model.

### *4.4. Coarse-to-fine strategy and the 'distance band'*

Although the 2-D distance map can be constructed efficiently by the Fast Marching Method, computation of the distance value in the entire region of the color image is wasteful. Therefore, we adopt a coarse-to-fine strategy and a band-shaped distance map, which is referred to as a distance band. The distance band is a narrow band along the image boundary and the precise distance map is constructed in this region using the Fast Marching Method. In regions other than the distance band, the distance value is roughly estimated as the distance from the center of the image boundary. In the beginning of the registration process, we use a coarse image and a wide distance band in order to align the 2-D image and the 3-D model roughly. After several iterations, we switch to the fine image and compute the distance band with a narrower width. In experiments, we used a distance band with 10 pixels and three images with different resolutions, namely $160 \times 120$, $320 \times 240$ and $640 \times 480$. The computation time of the distance band in each image is shown in Table 1.

**Table 1.**
Computation time of the distance band by the Fast Marching Method

| Image size | Entire region (ms) | Distance band (10 pixels) (ms) |
|---|---|---|
| $160 \times 120$ | 6.9 | 0.48 |
| $320 \times 240$ | 32.8 | 1.1 |
| $640 \times 480$ | 189.1 | 2.7 |

## 5. EXPERIMENTS

In this section, we present some fundamental results of the registration and tracking experiments using simulated images and actual images of the endoscopic operation.

### *5.1. The 2-D–3-D registration of simulated images*

First, Fig. 8 shows the application of proposed 2-D–3-D registration algorithm to a model of a small doll (height 5 cm). The boundary of the object on the 2-D color image is detected by applying the Level Set Method [13] to the background subtraction image.

The computation time of the force $f_i$ for one patch on the 3-D model is 0.30 μs for a 3.06-GHz Pentium IV processor. The total processing time is 9.6 ms for one update period, including projected contour detection, calculation of force and moment, and execution of the steepest descent method. The average and the variance of the registration error between the boundary and the projected contour are 1.19 pixels and 0.90 pixels$^2$, respectively, after 60 iterative calculations. Here,

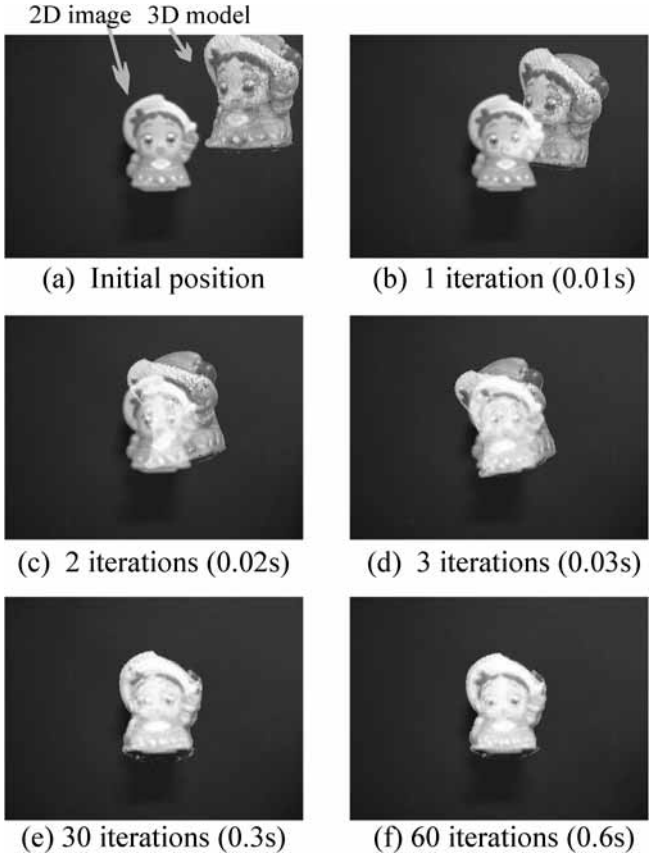


**Figure 8.** The 2-D–3-D registration of simulation images.

the number of points on the boundary is 652, the image size is $640 \times 480$ pixels and the 3-D model is composed of 73 192 meshes with 219 576 vertices. On the other hand, the computation time of force $f_i$ for the conventional point-based method [4] is 1.15 μs, which uses the $k$–$D$ tree structure to search the nearest points between the contour points of the 2-D image and the projected 3-D model.

Table 2 shows the comparison of the processing time for several cases in which different numbers of points on the boundary were used. From these results, it is clear that the processing time of the proposed method is approximately constant, even if the number of points on the boundary increases. On the other hand, the point-based approach requires a 3–7-times longer processing time than the proposed method. Moreover, the larger the number of points becomes, the longer the processing time required for the point-based approach. Therefore, it is verified that the proposed 2-D–3-D registration algorithm has an advantage compared with the conventional point-based approach in view of the execution time, especially when there are a large number of points on the boundary.

The next example is an experiment to examine the tracking of a moving object. Figure 9 shows the tracking results of a doll moving on the image plane. As seen in

**Table 2.**
Comparison of processing time for one patch

| Number of points on boundary | Proposed method (μs) | Point-based method [4] (μs) |
|---|---|---|
| 628 | 0.30 | 1.15 |
| 1265 | 0.30 | 1.50 |
| 1868 | 0.30 | 1.70 |
| 2490 | 0.30 | 2.22 |

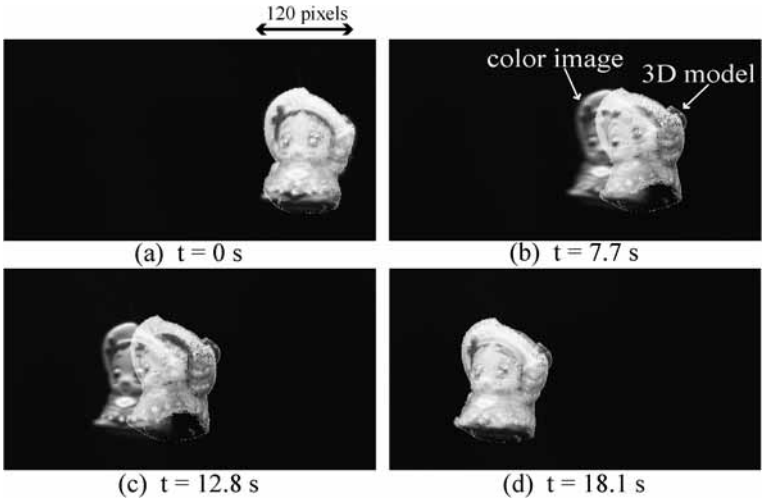


**Figure 9.** An example of moving object tracking.

this example, the 2-D–3-D registration can be performed even if the object moves up to 20.5 pixels/s. This result suggests that it is possible to overcome the registration error due to unknown disturbances, such as the breathing or heartbeat of the patient, in endoscopic images.

### *5.2. The 2-D–3-D registration using actual images of the endoscopic operation*

We carried out fundamental experiments for the navigation system of the endoscopic operation.

First, we attempted 2-D–3-D registration using actual endoscopic images of the liver phantom and the 3-D model. Figures 10 and 11 show the experimental setup and the 3-D model of the liver phantom constructed using the CT scanner. The oblique-viewing endoscope OTV-S5 (Olympus) is used for the experiments. An example of endoscopic images and the registration result are shown in Fig. 12a and 12b1. Figure 12b2 and 12b3 shows the superimposed images from some view points which are different from the view point used for the 2-D–3-D registration. The average error of contour lines is 8.06 pixels (8.24 mm at the position of the 3-D model) and the standard deviation is 5.94 pixels (5.46 mm).

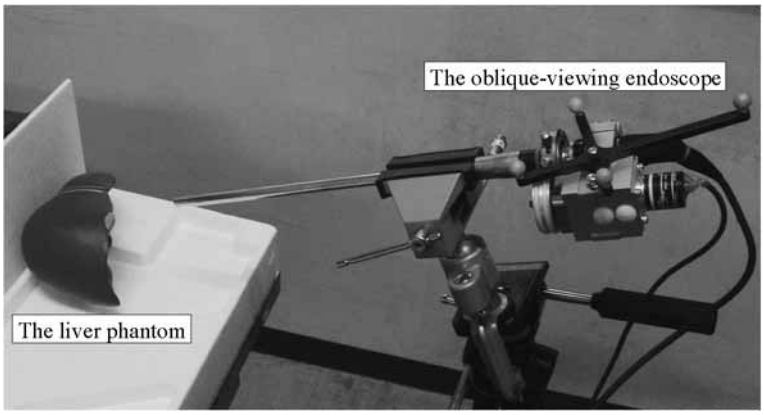


**Figure 10.** Experimental setup.

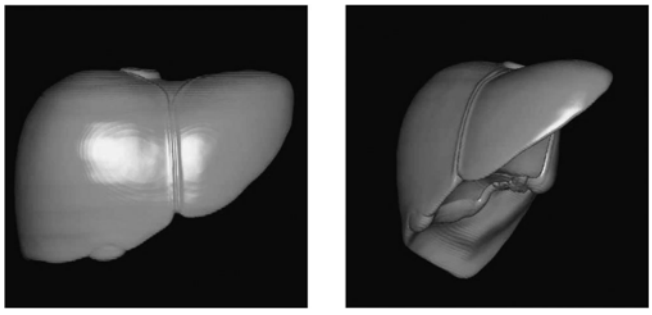

**Figure 11.** The 3-D liver phantom.

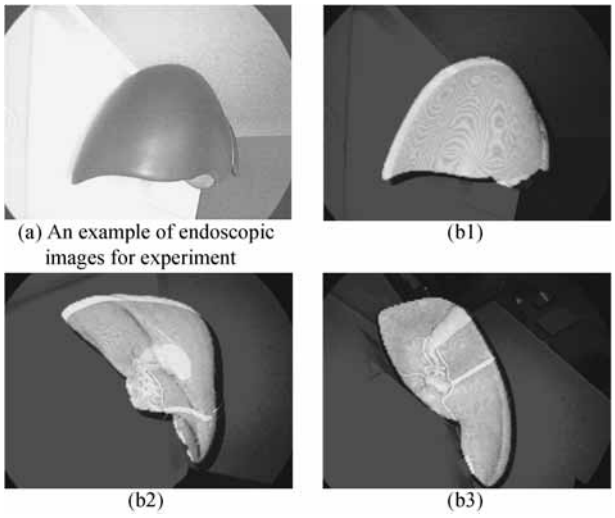


**Figure 12.** Superimposition of the 3-D liver phantom on the endoscopic images using a single endoscopic image.

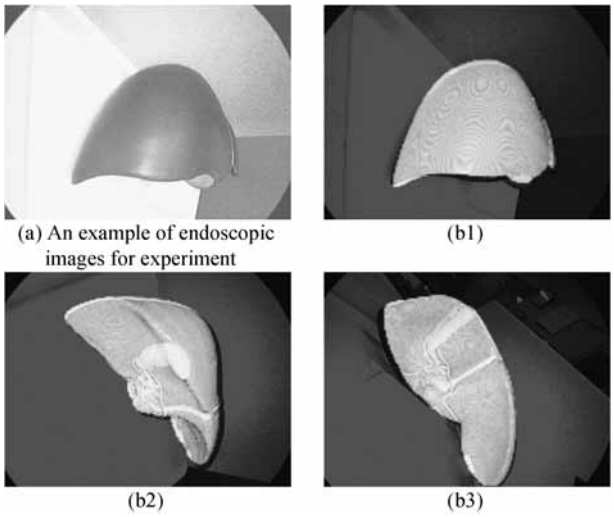


**Figure 13.** Superimposition of the 3-D liver phantom on the endoscopic images using four endoscopic images.

Figure 13 shows the registration results using four endoscopic images taken from four different view points, which are shown in Fig. 14. The average error of contour lines in this case is 5.40 pixels (4.97 mm) and the standard deviation is 3.98 pixels (3.66 mm), respectively. It is shown that the registration error is reduced using multiple images taken from different view points.

Next, we attempted 2-D–3-D registration using actual images of the endoscopic operation of cirrhosis of the liver. Figure 15 shows the initial results of the

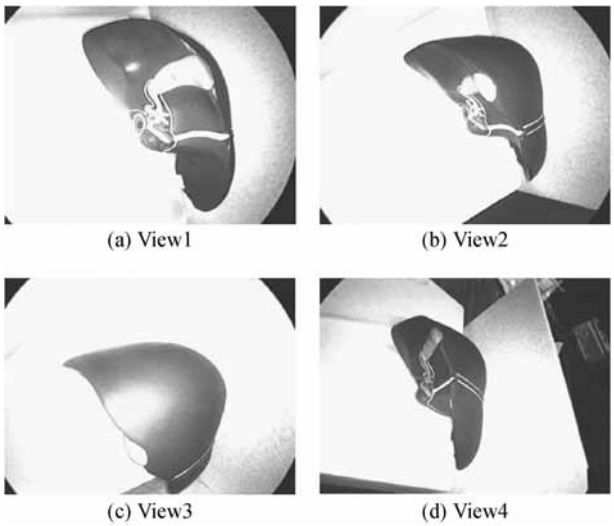


**Figure 14.** Four view points for the registration.

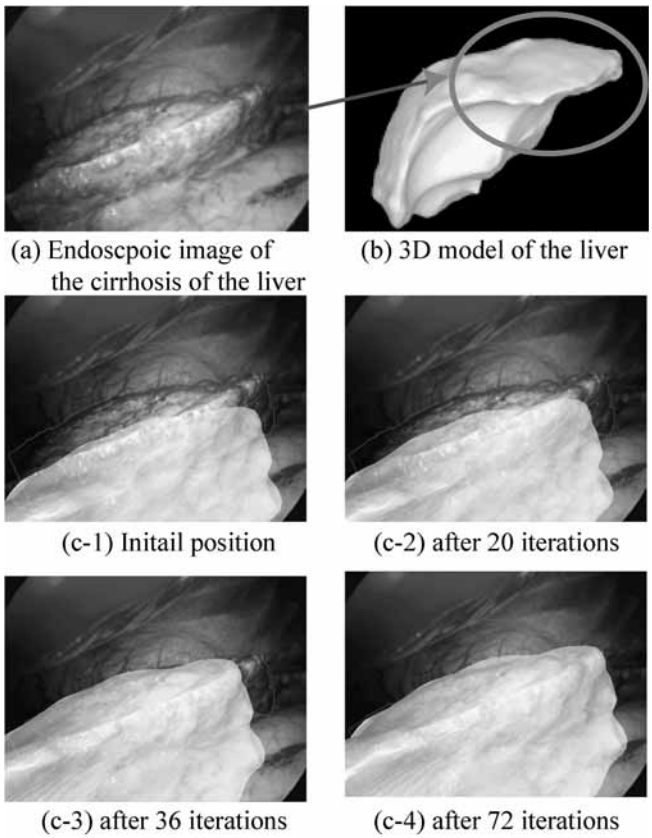


**Figure 15.** The 2-D–3-D registration using actual images of cirrhosis of the liver.

experiments. Figure 15a shows the actual image of the endoscopic operation of cirrhosis of the liver. In this image, the liver is partially hidden by the other organs. Figure 15b and 15c shows the 3-D model of the liver obtained from the CT images and some experimental results for the 2-D–3-D registration, respectively. The registration is successfully executed if the initial position of the 3-D model is sufficiently close to the image of cirrhosis of the liver.

Figure 16 shows the tracking results for the gallbladder in video images taken by the endoscope. The boundaries of the gallbladder on every 2-D video image are detected using Snakes. As seen in this result, the proposed algorithm can track the gallbladder even if the gallbladder image moves due to changes in the position of the endoscope.

Through the series of experiments, the proposed algorithm performs tracking of organs in endoscopic images within 30 ms in processing time and 10 mm in

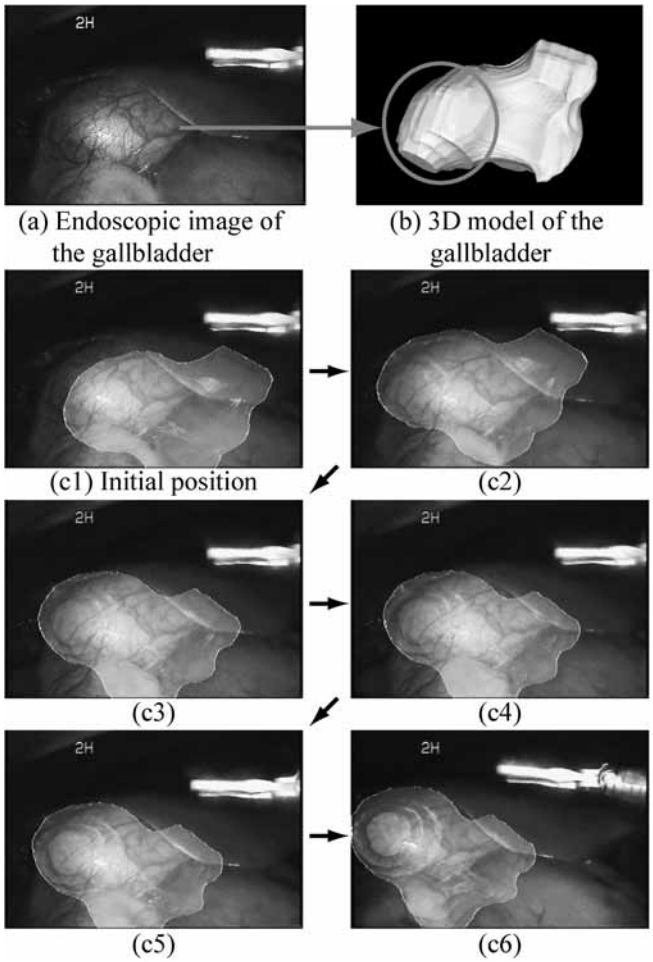


**Figure 16.** The 2-D–3-D registration in endoscopic video images of the gallbladder.

accuracy in many cases. Although the current performance, especially the accuracy, is not always sufficient for image-guided surgery, we think the approximate position of a tumor can be presented for an operator and it is quite helpful for intuitive understanding of the operating procedure. We will improve the performance of the system by combining the information from other sensors such as magnetic sensors or ultrasonic probes in the future.

## 6. CONCLUSIONS

The present paper describes a new registration algorithm of 2-D color images and 3-D geometric models for the navigation system of a surgical robot. This method utilizes the 2-D images and their distance map created by the Fast Marching Method, and determines the precise relative positions of 2-D images and 3-D models. The efficiency of the proposed algorithm was verified through the fundamental experiments using simulation images and actual images of an endoscopic operation of liver.

We have conducted experiments with various images and 3-D models, and have obtained good results. Occasionally, the performance of the proposed algorithm is reduced, especially in cases in which only the partial edge of an organ is visible from the endoscope. However, once registration is successfully performed, the algorithm can track a moving object stably and continuously. Therefore, the proposed algorithm is quite useful for developing a practical navigation system since it overcomes the registration error caused by organ movement due to unknown disturbances such as the breathing or heartbeat of the patient.

*Acknowledgments*

This research was supported in part by the 21st Century COE Program 'Reconstruction of Social Infrastructure Related to Information Science and Electrical Engineering', and by the Ministry of Public Management, Home Affairs, Posts and Telecommunications of Japan under the Strategic Information and Communications R&D Promotion Program (SCOPE).

## REFERENCES

1. M. Hashizume, M. Shimada, M. Tomikawa, Y. Ikeda, I. Takahashi, R. Abe, F. Koga, N. Gotoh, K. Konishi, S. Maehara and K. Sugimachi, Early experiences of endscopic procedures in general surgery assisted by a computer-enhanced surgical system, *Surg. Endosc.* **16**, 1187–1191 (2002).
2. P. Viola and W. W. III, Alignment by maximization of mutual information, *Int. J. Comput. Vis.* **24**, 137–154 (1997).
3. I. Stamos and P. K. Allen, Integration of range and image sensing for photorealistic 3d modeling, in: *Proc. IEEE Int. Conf. on Robotics and Automation*, San Francisco, CA, pp. 1435–1440 (2000).

4. R. Kurazume, K. Noshino, Z. Zhang and K. Ikeuchi, Simultaneous 2D images and 3D geometric model registration for texture mapping utilizing reflectance attribute, in: *Proc. 5th Asian Conf. on Computer Vision*, Melbourne, pp. 99–106 (2002).
5. M. D. Elstrom and P. W. Smith, Stereo-based registration of multi-sensor imagery for enhanced visualization of remote environments, in: *Proc. IEEE Int. Conf. on Robotics and Automation*, Detroit, MI, pp. 1948–1953 (1999).
6. K. Umeda, G. Godin and M. Rioux, Registration of range and color images using gradient constraints and range intensity images, in: *Proc. 17th Int. Conf. Pattern Recognition*, Cambridge, pp. 12–15 (2004).
7. H. Lensch, W. Heidrich and H.-P. Seidel, Automated texture registration and stitching for real world models, in: *Proc. Pacific Graphics*, Hong Kong, pp. 317–326 (2000).
8. H. Lensch, W. Heidrich and H. P. Seidel, Hardware-accelerated silhouette matching, in: *Proc. SIGGRAPH Sketches*, New Orleans, LA (2000).
9. K. Matsushita and T. Kaneko, Efficient and handy texture mapping on 3D surfaces, *Comput. Graphics Forum* **18**, 349–358 (1999).
10. P. J. Neugebauer and K. Klein, Texturing 3D models of real world objects from multiple unregistered photographic views, *Comput. Graphics Forum* **18**, 245–256 (1999).
11. J. Sethian, A fast marching level set method for monotonically advancing fronts, *Proc. Natl. Acad. Sci. USA* **93**, 1591–1595 (1996).
12. J. Sethian, *Level Set Methods and Fast Marching Methods*, 2nd edn. Cambridge University Press, Cambridge (1999).
13. Y. Iwashita, R. Kurazume, T. Tsuji, K. Hara and T. Hasegawa, Fast implementation of level set method and its realtime applications, in: *IEEE Int. Conf. on Systems, Man and Cybernetics*, The Hague, pp. 6302–6307 (2004).

## ABOUT THE AUTHORS

**Yumi Iwashita** received her MS degree from the Graduate School of Information Science and Electrical Engineering, Kyushu University, in 2004. She is a Research Fellow of the Japan Society for the Promotion of Science. She is currently working on the development of surgical navigation systems as a PhD candidate of the Graduate School of Information Science and Electrical Engineering, Kyushu University.

**Ryo Kurazume** received his ME and BE degrees from the Department of Mechanical Engineering Science, Tokyo Institute of Technology, in 1991 and 1989, respectively. His PhD degree was from the Department of Mechanical Engineering Science, Tokyo Institute of Technology, in 1998. He is an Associate Professor at the Graduate School of Information Science and Electrical Engineering, Kyushu University. His current research interests include multiple mobile robots, 3-D modeling, manipulator, walking robots and medical image analysis.

**Kozo Konishi** received the PhD from the Graduate School of Medical Sciences, Kyushu University, in 2005. He is currently an Associate Researcher of Center for Integration of Advanced Medicine and Innovative Technology, Kyushu University.

**Masahiko Nakamoto** received his BS, MS and PhD degrees in Information and Computer Sciences from Osaka University, Japan in 1997, 1999 and 2002, respectively. In 2005, he joined the Division of Image Analysis of Osaka University Graduate School of Medicine as a Faculty Member. He is currently an Assistant Professor at Osaka University Graduate School of Medicine and an Adjunct Assistant Professor at the Graduate School of Information Science and Technology, Osaka University, where he is working on the development of surgical navigation systems in the Division of Image Analysis.

**Naoki Aburaya** received the BS degree in Information and Computer Sciences from Osaka University, in 2005. He is currently working on the development of endoscopic surgical navigation systems in the Division of Image Analysis, Osaka University Graduate School of Medicine as a graduate student of Graduate School of Information Science and Technology, Osaka University.

**Yoshinobu Sato** received his BS, MS and PhD degrees in Information and Computer Sciences from Osaka University, in 1982, 1984 and 1988 respectively. From 1988 to 1992, he was a Research Engineer at the NTT Human Interface Laboratories. In 1992, he joined the Division of Functional Diagnostic Imaging of Osaka University Medical School as a Faculty Member. From 1996 to 1997, he was a Research Fellow in the Surgical Planning Laboratory, Harvard Medical School and Brigham and Women's Hospital. He is currently an Associate Professor at Osaka University Graduate School of Medicine and an Adjunct Associate Professor at the Graduate School of Information Science and Technology, Osaka University, where he leads a group conducting research on 3-D image analysis and surgical navigation systems in the Division of Image Analysis.

**Makoto Hashizume** received the PhD and MD degrees from the Graduate School of Medical Sciences, Kyushu University, in 1979 and 1984, respectively. He is currently a Professor and Chairman, Department of Disaster and Emergency Medicine, Graduate School of Medical Sciences, Kyushu University and Director, Center for Integration of Advanced Medicine and Innovative Technology. He is a General Surgeon and has a lot of clinical experience with robotic surgery with 'da Vinci'. He has been developing a MR compatible surgical robotic system as a project leader collaborating with several companies and engineering departments of other universities in Japan.

**Tsutomu Hasegawa** received the BE degree in Electronic Engineering and the PhD degree both from the Tokyo Institute of Technology, in 1973 and 1987, respectively. He was associated with the Electrotechnical Laboratory of the Japanese Government from 1973 to 1992, where he performed research in robotics. From 1981 to 1982, he was a Visiting Researcher at the Laboratoire d'Automatique et d'Analyses des Systemes (LAAS/CNRS), Toulouse, France. He joined Kyushu University, Fukuoka, in 1992, and is currently a Professor with the Department of Intelligent Systems, Graduate School of Information Science and Electrical Engineering, Kyushu University. His research interest are in manipulator control, geometric modeling and reasoning, motion planning, and man–machine interaction. He received the Franklin V. Taylor Memorial Award from the IEEE Systems, Man and Cybernetics Society in 1999.